B-T-3295

The Spectral Emittance and Stability of Coatings and Textured Surfaces for Thermophotovoltaic (TPV) Radiator Applications

B.V. Cockeram and J. L. Hollenbeck

USDOE contract No. DE-AC11-98PN38206

BETTIS ATOMIC POWER LABORATORY WEST MIFFLIN, PENNSYLVANIA 15122-0079

Operated for the U.S. Department of Energy
by Bechtel Bettis, Inc.

DISCLAIMER

The Spectral Emittance and Stability of Coatings and Textured Surfaces for Thermophotovoltaic (TPV) Radiator Applications

B.V. Cockeram and J. L. Hollenbeck

Bechtel-Bettis Atomic Power Laboratory
P.O. Box 79
West Mifflin, PA 15122-0079

Abstract

Coatings or surface modifications are needed to improve the surface emissivity of materials under consideration for TPV radiator applications to a value of 0.8 or higher. Vacuum plasma spray coatings (ZrO_2 + 18% TiO_2 + 10% Y_2O_3, ZrC, Fe_2TiO_5, $ZrTiO_4$, ZrO_2 + 8% Y_2O_3 + 2% HfO_2, and Al_2O_3 + TiO_2) and a chemical vapor deposited coating of rhenium whiskers were used to increase the surface emissivity of refractory metal and nickel-base materials. Emittance measurements following 4000 hours of vacuum annealing at 1100°C show that only the ZrO_2 + 18% TiO_2 + 10% Y_2O_3, ZrC, and Al_2O_3 + TiO_2 coatings have the desired thermal stability, and maintain emissivity values higher than 0.8. These coatings are graybody emitters, and provide a high emissivity value in the wavelength range that is relevant to the TPV cells. The highest emissivity values were observed for the Al_2O_3 + TiO_2 coatings, with post-anneal values higher than graphite.

Introduction

A radiator is required for a thermophotovoltaic (TPV) power generation system to convert heat into infrared (IR) photons that are emitted to TPV cells that directly convert the radiant energy into electrical power. Emissivity is a relative measure of the efficiency of photon radiation from a surface, with a value of 1.0 being the maximum for a perfect black body. Metallic alloys that could be used as TPV radiator structural materials (molybdenum-, niobium-, and nickel-base alloys) have an inherently low emissivity (~0.12 to 0.4). Previous work has focused on two approaches for increasing the surface emissivity [1]: (1) application of a coating material that has a high emissivity, and (2) surface modification of the radiator materials to create high aspect ratio features (or cavities) to increase emissivity. Emissivity enhancement coatings are attractive because these layers could also serve as a protective barrier and limit oxidation in accident conditions where air and/or water ingress could occur. Surface modification approaches have the advantage that coating/substrate interactions and coating stability concerns are eliminated.

A number of coatings and surface modification approaches were previously evaluated, and seven prime candidates were shown to be thermally stable for at least 500 hours at 1100°C and increase the surface emissivity of molybdenum-, niobium- and nickel-base materials to at least 0.8 or higher [1]. Six candidates were vacuum plasma spray coatings (ZrO_2 + 18% TiO_2 + 10% Y_2O_3, ZrC, Fe_2TiO_5, $ZrTiO_4$, ZrO_2 + 8% Y_2O_3 + 2% HfO_2, and Al_2O_3 + TiO_2). One candidate was a surface modification consisting of a chemical vapor deposited (CVD) coating of rhenium whiskers. These coatings were also resistant to thermal cycling damage resulting from rapid cooling from 1100°C.

Since the TPV radiator must operate at temperatures greater than 950°C for periods of time longer than 500 hours, the thermal stability of emissivity enhancement coatings was evaluated after vacuum annealing at 1100°C to 1500°C for 500 to 6000 hours. The thermal stability of the coatings was evaluated by weight loss measurements, metallographic examinations, and emissivity measurements after vacuum annealing at 1100°C. Spectral emissivity data was evaluated to determine the effectiveness of the coatings in the wavelength range that matches the bandgap of the TPV cells.

Coatings and Experimental Procedures

The coatings and/or surface modifications were applied to discs that were 2.54 cm diameter X 0.15 cm thick with surface roughness of $R_a < 8$ μ-inch. Four base-materials were coated [1]: (1) arc cast , commercially pure (CP) molybdenum (ASTM B387-90 Type 361 SR), (2) an oxide dispersion strengthened (ODS) molybdenum alloy, (3) CP electron-beam melted niobium (ASTM B392-89 Type 2), and (4) the nickel-base alloy Haynes 230.

Five coatings (ZrO_2 + 18% TiO_2 + 10% Y_2O_3, ZrC, Fe_2TiO_5, $ZrTiO_4$, and ZrO_2 + 8% Y_2O_3 + 2% HfO_2) were deposited on molybdenum, niobium, and Haynes 230 by Vacuum Plasma Spray (VPS) at the Thermal Spray Laboratory at the State University of New York at Stony Brook (SUNY). Two coating layers were deposited to a total nominal coating thickness of 50-75 μm: (1) a 25 μm thick bond coat consisting of a 50/50 mixture of substrate powder (molybdenum, niobium, or Haynes 230) and coating powder, and (2) a 25-50 μm thick top layer of coating material. The substrate powder additions were made to minimize the differences in coefficient of thermal expansion (CTE) between the coating and substrate and to improve adhesion.

Alumina - titanium dioxide (Al_2O_3 + TiO_2) coatings were deposited on molybdenum and niobium substrates by Praxair Surface Technologies, Indianapolis, Indiana using VPS (25-50 μm thick) and detonation gun (D-gun, for coatings 25-50 μm and 125-175 μm thick) methods. In all cases, the coatings that contain multiple oxides were produced by blending the constituent powders prior to deposition. A range of the Al_2O_3 + TiO_2 coating compositions were deposited on molybdenum and niobium in batches of twelve to eight discs using a Sultzer-Metco Low-Pressure Plasma Spray (LPPS) system at Bettis. All powders used for coating ranged in size from 25 μm to 5 μm and were fused by passing the powder particles through a plasma torch to produce a more spherical shape with better flow characteristics. Pre-blended powders of $97Al_2O_3$ / $3TiO_2$, $87Al_2O_3$ / $13TiO_2$, and $60Al_2O_3$ / $40TiO_2$ (all compositions given in weight%) were formed at F.J. Brodmann & Co., Harvey, LA, by mixing pure Al_2O_3 and TiO_2 powders to the desired composition, and then fusing (passing the particles through a plasma torch) to produce powder particles that are chemically mixed. Other powder compositions ($90Al_2O_3$ / $10TiO_2$, $85Al_2O_3$ / $15TiO_2$, $80Al_2O_3$ / $20TiO_2$, and $75Al_2O_3$ / $25TiO_2$) were formed by weighing pure Al_2O_3 and TiO_2 powders to the desired composition.

CVD rhenium whiskers were deposited on molybdenum substrates by Ultramet Inc., Pocoima, CA. The use of varying CVD deposition times had a marked effect on the whisker morphology [1].

Emissivity was determined at NASA Glenn Research Center (NASA-GRC) by measuring spectral reflectance at room temperature, which was used to determine room-temperature spectral emittance values with the assumption of zero transmittance via Kirchoff's Law (emittance = 1 – reflectance) [2,3]. Hemispherical reflectance values were obtained as a function of wavelength from 0.25 to 2.5 μm using a Perkin Elmer Lambda-19 spectrophotometer with a Labsphere integrating sphere attachment. Hemispherical reflectance as a function of wavelength from 2.0 to 25 μm was measured using a Surface Optics SOC-400. Data corrections are made for each instrument using a Spectralon standard for the Lambda-19 and gold standard for the SOC-400. The results from the Lambda-19 and SOC-400 are meshed together by weighting the averages in the 2.0 to 2.5 μm range to yield a single data set covering the wavelength range from 0.25 to 25 μm range. Total (wavelength = 0.25 to 25 μm) hemispherical (solid angle approximately equal to π) emittance at room-temperature was calculated from the spectral emittance data obtained from both instruments. It is assumed that the spectral emittance at room-temperature is an approximate measure of the total hemispherical emittance at high temperatures and the optical properties of the material are not significantly changed at high temperatures [2]. The total hemispherical emittance at a given temperature ($\varepsilon(T_A)$) is determined from the measured spectral emittance data (ε_λ) at room-temperature (T) and the black body distribution function ($\varepsilon_{\lambda b}$) at the temperature of interest (T_A) using the following equation

$$\varepsilon(T_A) = \frac{\int_{0.25\,\mu m}^{25\,\mu m} \varepsilon_\lambda(\lambda, T)\,\varepsilon_{\lambda b}(\lambda, T_A)\,d\lambda}{\sigma T_A^4} \qquad (1)$$

where ε_λ is the spectral emittance at a wavelength λ, and σ is the Stefan Boltzmann constant [4].

The thermal stability of the coatings was evaluated by exposing the coupons to a dynamic vacuum ($< 10^{-5}$ torr) anneal at 1100°C, 1200°C, 1350°C, or 1500°C for 500 to 6000 hours. For the coated substrates annealed at 1100°C, the total hemispherical emittance was measured in the pre- and post-anneal conditions. The weight change of all coatings was measured after vacuum annealing. Post-anneal metallographic, X-ray Diffraction (XRD), and Scanning Electron Microscopy (SEM) examinations were used to evaluate the thermal stability of the coatings.

Results and Discussion

$Al_2O_3 + TiO_2$ Coatings

The spectral emissivity values for the VPS $Al_2O_3 + TiO_2$ coatings are shown in Figure 1a to be slightly higher at the low wavelengths. Similar trends were observed for the spectral emissivity values of other $Al_2O_3 + TiO_2$ coatings. The $Al_2O_3 + TiO_2$ coatings are essentially graybody emitters, which means there is little change in spectral emissivity as a function of wavelength. This means that total emissivity values that are integrated over the whole wavelength range are a reasonable measure of spectral emittance. Little change in spectral emissivity values are shown in Figure 1a after vacuum annealing at 1100°C to 4000 hours in the wavelength range of 0.25 to 11 μm, which indicates that these coatings are stable.

Figure 1b shows that vacuum annealing of the VPS $Al_2O_3 + TiO_2$ coatings deposited on molybdenum for up to 4000 hours resulted in no significant change in emittance. A small decrease in emissivity was observed for the VPS coating deposited on niobium, but these values were constant after 2000 hours of annealing at 1100°C. The VPS coatings deposited on niobium contained a low level of niobium, and the formation of niobium containing oxides, which are known to have a lower emissivity than Al_2O_3 or TiO_2 [5], may have resulted in this decrease in emissivity.

The emissivity values for the D-gun $Al_2O_3 + TiO_2$ coatings showed a slight decrease and then a subsequent increase with annealing time, which resulted in little net change in emissivity at the end of the annealing period. The post-anneal emissivity values for the D-gun coatings were higher than the values for as-received Poco graphite while the values for the VPS coatings were comparable to Poco graphite. XRD analysis showed that the as-deposited coatings consisted of TiO_2 (Rutile) and Al_2O_3 with the α and γ polymorphs for the VPS coating and γ and χ polymorphs for the D-gun coatings [1]. After 500 hours of annealing, both the VPS and D-gun coatings consisted of α-Al_2O_3 with alumina-titanate phases (e.g. $Al_2Ti_7O_{15}$). Further phase changes and conversion into titanate phases during vacuum annealing may produce the initial decrease and then increases in emissivity to give the stable emissivity values in Figure 1b. Low weight changes were observed after vacuum annealing at 1100°C to 1200°C for times up to 6000 hours. Figures 2a and 2b show that little change in coating microstructure is observed after vacuum annealing at 1200°C. The coating has the same lamellar structure of Al_2O_3 and TiO_2 layers that is observed in the as-deposited coatings [1], and no change in porosity is observed. Coating / substrate interactions are not observed, as confirmed by the post-anneal hardness profiles that show no hardness gradient with baseline hardness values comparable to uncoated controls. Higher weight losses and the formation of pores are observed after vacuum annealing at 1350°C to 1500°C. These weight losses result from the higher vapor pressure of TiO_2 in vacuum conditions. However, the Al_2O_3 / TiO_2 coatings exhibit excellent thermal stability at 1200°C, which is well above most application temperatures, and provide post-anneal emissivity values that are comparable to or greater than that for Poco Graphite.

A thermodynamic computation software program (HSC Chemistry [6]) was used to calculate equilibrium vapor pressures for Al_2O_3 and TiO_2, see Table I. The Hertz-Langmuir equation is used to calculate the rate of evaporation (J, in collisions /cm^3)

$$J = (P) / (2\pi mkT)^{1/2} \qquad (2)$$

Where P is the partial pressure of the gas phase species with the highest vapor pressure, m is the molecular weight of this gas phase species, k is the Boltzman constant, and T is absolute temperature [7]. Converting this expression into practical units for evaporation rate (G in grams / cm^2 -s),

$$G = (\alpha P_{torr}) / (17.14(T/m)^{1/2}) \qquad (3)$$

where P_{torr} is the vapor pressure of the most volatile species in units of torr. The Hertz-Langmuir rate is the maximum possible evaporation rate that is theoretically predicted for a solid, and is typically an over-estimate for most materials. In most practical applications the evaporation is less than the value predicted by Eq. (3) by a de-absorption constant (α) that typically ranges from 10^{-2} to 10^{-6}, and must be experimentally determined [7]. The most volatile vapor species for Al_2O_3 (AlOH(g)) would result in evaporation rates that are much less than indicated by the observed weight losses, while the higher rate for TiO_2 (TiO_2(g)) would produce a significantly higher weight loss than measured. This indicates that some limited evaporation of TiO_2 could produce the low weight losses, but the metallographic evidence and lack of change in emissivity values with annealing indicate that the Al_2O_3 - TiO_2 coating has excellent thermal stability.

Metallographic examination shows in Figures 2c and 2d that the as-deposited LPPS coatings generally had only a small amount of porosity that was not interconnected. The LPPS Al_2O_3 / TiO_2 coatings that were produced from pre-blended and fused feedstocks ($97Al_2O_3$ / $3TiO_2$ and $87Al_2O_3$ / $13TiO_2$) had a more homogeneous, finer, and lamellar grain structure with few defects (Figure 2c). The LPPS coatings that were produced from mixed $Al_2O_3 + TiO_2$ feedstocks ($90Al_2O_3$ / $10TiO_2$, $85Al_2O_3$ / $15TiO_2$, $80Al_2O_3$ / $20TiO_2$, and $75Al_2O_3$ / $25TiO_2$) were observed to contain cracks in the

coating layer and spherical particles (Figure 2d). A higher density of defects was observed in the coatings of higher TiO_2 content, which may be the result of CTE differences between the Al_2O_3 + TiO_2 phases. Previous thermal cycle testing showed that the VPS and D-gun coatings had excellent thermal cycle damage resistance [1]. The weight changes for the LPPS coatings were comparable to or less than the uncoated controls and the VPS and D-gun coatings. No evidence of coating spalling was observed, which indicates that the LPPS coatings also had excellent resistance to damage from thermal cycling. Cracks were observed on the surface of LPPS coatings produced from the mixed Al_2O_3 + TiO_2 feedstocks ($90Al_2O_3$ / $10TiO_2$, $85Al_2O_3$ / $15TiO_2$, $80Al_2O_3$ / $20TiO_2$, and $75Al_2O_3$ / $25TiO_2$). Although cracks were observed, these LPPS coatings were tightly adherent and did not spall. Cracks were not observed in the $97Al_2O_3$ / $3TiO_2$ and $87Al_2O_3$ / $13TiO_2$ LPPS coatings produced from pre-blended and fused feedstocks, which indicates that these coatings are more resistant to damage from thermal cycling. The finer and more homogeneous grain structure of the coatings produced from pre-blended and fused feedstocks (Figure 2c) likely produces the improved damage resistance. Cracking observed on the surface of the LPPS $60Al_2O_3$ / $40TiO_2$ coating after thermal cycling, which was produced from a pre-blended and fused feedstock, was likely produced by the higher TiO_2 content of the coating and resulting stresses from CTE differences.

The total hemispherical emittance (Figure 3) and spectral emissivity values for all Al_2O_3 – TiO_2 coatings in the as-deposited condition were independent of substrate type. The variation of emissivity values with respect to the TiO_2 content of the Al_2O_3 – TiO_2 coatings was shown in Figure 3 to be fairly small. The following points summarize the trends observed for both the total hemispherical emittance and spectral emissivity values of the Al_2O_3 + TiO_2 coatings in the as-deposited condition: (1) the highest emissivity values were observed for the D-gun coatings, (2) the lowest emissivity values were observed for the VPS coatings, (3) emissivities of the LPPS Al_2O_3 – TiO_2 coatings were within the range of values for the VPS and D-gun coatings, and (4) for the LPPS coatings, slightly higher emissivity values were observed for the $90Al_2O_3$ / $10TiO_2$ and $85Al_2O_3$ / $15TiO_2$ coatings produced from mixed powder feedstocks. Although post-anneal emissivity values have not been obtained for the LPPS coatings, the as-deposited emissivity values are higher than Poco graphite and within the range of the VPS and D-gun coatings, which have post-anneal emissivity values higher than graphite (Figure 1b).

ZrC Coatings

The emissivity values for the as-deposited ZrC coatings were found to be independent of substrate and very reproducible for duplicate coatings (Figures 4 and 5), even though the VPS ZrC coatings contained a significant volume fraction of substrate particles [1]. Spectral emissivity values for the ZrC coatings are shown in Figure 4 to be slightly higher in the lower wavelength range with a slight decrease in emissivity at higher wavelengths. However, the spectral emissivity values for the ZrC coatings were relatively constant as a function of wavelength, which indicates that these coatings are graybody emitters.

As-deposited emissivity values for the ZrC coating were higher than Poco graphite. Vacuum annealing of the ZrC coatings is shown in Figure 5 to produce a sharp initial decrease in emissivity (0.91-0.89 for as-deposited to 0.85-0.84 after 1100°C/500h vacuum anneal). Further vacuum annealing at 1100°C to 4000 hours resulted in little change in emissivity (0.85-0.84 for 1100°C/500h to 0.84-0.83 for 1100°C/4000h) and little weight change, which shows that the ZrC coatings have good long-term stability after the initial thermal exposure. Post anneal spectral emissivity curves for the ZrC coating are shifted to lower values compared to the as-deposited data in Figure 4, but the trend in spectral emissivity curves was not changed with annealing. The post-

anneal emissivity values for the ZrC coating are only slightly less than the as-received values for Poco graphite.

Previous SEM examinations of the ZrC coating showed that these deposits contained substrate particles [1]. The metallographic cross-section of the as-deposited coating shows in Figure 6a that the ZrC coating is fairly thin (15 μm to 25 μm) and the coating contains a fairly high fraction of niobium substrate particles for the coating deposited on niobium. Similar features were observed for the ZrC coating deposited on molybdenum (Figure 6b) and Haynes 230. XRD analysis of the as-deposited ZrC coatings confirmed that these layers are primarily ZrC [ICDD Card # 19-1487] with substrate particles. Metallography of the ZrC coating deposited on molybdenum following a 1200°C/6000h anneal shows in Figure 6b that coating/substrate interactions had not occurred, and the coating thickness was not changed. No increase in micro-hardness values was detected in profiles taken near the coating/substrate interface, and the hardness values were comparable to baseline values for uncoated controls, which also confirmed that substrate/coating interactions had not occurred. Post-anneal XRD analysis showed that the coating was primarily ZrC with a slight shifting in lattice parameter, and ZrO_2 was detected. For the ZrC coating deposited on molybdenum, molybdenum substrate particles were not detected after vacuum annealing, which indicates that the formation of volatile molybdenum-oxides had removed these particles [1]. The initial weight loss and decrease in emissivity observed within the first 500 hours of vacuum annealing probably results from slight oxidation of the ZrC coating at low oxygen partial pressure (P_{O2}) to form a ZrO_2 scale and CO or CO_2 gas, and oxidation/reaction of the substrate particles in the ZrC coating. The ZrO_2 scale is too thin to be resolved in Figure 6b. ZrO_2 scales formed at low P_{O2} are typically adherent, compared to ZrO_2 scales formed in air. Vacuum annealing at 1200°C to 1500°C also showed an initial weight loss after the initial 500h period, with little weight change from 500h to 6000h of annealing time (weight changes comparable to the Al_2O_3 – TiO_2 coatings). Vacuum annealing at 1200°C to 1500°C produced no significant thinning or porosity formation for the ZrC coating deposited on molybdenum, which indicates that this coating is thermally stable. The evaporation rate for ZrC is predicted in Table I to be very high, while the lowest evaporation rate is calculated for ZrO_2. This indicates that the formation of the ZrO_2 scale probably protects the ZrC coating to result in excellent thermal stability in vacuum.

For the ZrC coating deposited on niobium, coating/substrate interactions were observed after vacuum annealing with the formation of Nb-carbide precipitates at the coating substrate interface. Post-anneal XRD analysis also confirmed the presence of niobium-carbides for the ZrC coating deposited on niobium. The thermodynamic stability of ZrC is comparable to Nb_2C; at 1200°C the Gibbs energy of formation for ZrC is –184.2 KJ/mol and for Nb_2C is –175.2 KJ/mol [8]. Since ZrC has a wide range of composition, which would vary the Gibbs energy of formation, various ZrC stoichiometries may exist in the coating that could be slightly less stable than Nb_2C to result in the formation of Nb_2C precipitates in the niobium substrate with vacuum annealing. Post-anneal metallographic examinations showed thinning of the ZrC coating, and the formation of large niobium-carbide precipitates that increase the hardness of the niobium substrate. This indicates that the ZrC coating should not be used on niobium substrates for TPV radiator applications. However, the emissivity values for the ZrC on molybdenum coating are stable from the 500 hour to 4000 hour period of annealing time and only slightly lower than values for as-received graphite, the ZrC coating on molybdenum is a reasonable choice for TPV radiator applications.

<u>ZrO_2 + 18% TiO_2 + 10% Y_2O_3 and ZrO_2 + 8% Y_2O_3 + 2% HfO_2 Coatings</u>

The ZrO_2 + 18% TiO_2 + 10% Y_2O_3 (ZTY) and ZrO_2 + 8% Y_2O_3 + 2% HfO_2 (ZYH) coatings contained a low volume fraction of substrate particles [1], the emissivity values for the as-deposited

coatings were independent of substrate and very reproducible for duplicate coatings, see Figure 5. The spectral emissivity values for the ZTY coatings were slightly less in the lower wavelength range with a slight peak in values at a wavelength of 11 μm to 13 μm followed by a decrease in emissivity values at wavelengths > 13 μm. The spectral emissivity values for the ZTY coatings were fairly constant as a function of wavelength, and these coatings are graybody emitters.

As-deposited emissivity values for the ZTY coating were comparable to Poco graphite. Vacuum annealing of the ZTY coatings at 1100°C for 4000h produced no change in emissivity (0.89-0.86 for as-deposited to 0.87 after 1100°C/4000h), see Figure 5. Little change in the spectral emissivity of the ZTY coatings was observed after vacuum annealing in Figure 7. The post-anneal emissivity values were independent of substrate type. This indicates that the ZTY coatings have excellent thermal stability under vacuum annealing conditions.

The as-deposited ZTY coating is shown in Figure 8a to be a fairly thick layer (50 μm to 80 μm) that appears to consist of more than one phase. Some porosity was observed in the as-deposited ZTY coatings in Figure 8a, which could result from metallographic preparation. XRD analysis indicated that the as-deposited ZTY coating was primarily ZrO_2 [ICDD card # 37-1484] with trace amounts of Y_2O_3 and TiO_2 that were not in solution in the ZrO_2 phase. Few substrate particles are observed in the ZTY coating, which may contribute to the excellent thermal stability. The weight change values observed for the ZTY coating with vacuum annealing at 1100°C to 1200°C were lower than observed for the ZrC and $Al_2O_3 - TiO_2$ coatings, and comparable to the uncoated substrates. The metallographic section of the ZTY coating after the 1200°C/6000h annealing shows in Figure 8b that the thickness and porosity was comparable to the as-deposited coating (Figure 8a). Post-anneal XRD analysis shows that the ZTY coating is primarily ZrO_2 [ICDD card # 37-1484] with trace amounts of Y_2O_3 and TiO_2 , which is identical to the as-deposited coating. Since the ZTY coatings are based on ZrO_2, which is a very stable oxide that has an inherently low evaporation rate at high temperatures in vacuum (Table I), the excellent thermal stability of these coatings is not surprising. No coating/substrate interactions were observed for either the molybdenum or niobium substrates after vacuum annealing at 1100°C to 1200°C, which indicates that the ZTY coating has excellent thermal stability. Some formation of coating porosity was observed after vacuum annealing at 1350°C with more porosity observed after vacuum annealing at 1500°C, which probably results from the evaporation of the Y_2O_3 and TiO_2 that is contained within the ZTY coating (Table I). The TPV radiator application temperature is far below 1350°C, and the thermal stability of the ZTY coating is considered to be excellent. Since the post-anneal emissivity values for the ZTY coating are comparable to as-received values for Poco graphite (Figure 5), and since little change in the emissivity values of the ZTY coatings were observed after vacuum annealing at 1100°C for 4000 hours, ZTY is a potential coating for TPV radiator applications.

The as-deposited emissivity values for the ZYH coating were less than Poco graphite. The spectral emissivity values for the ZYH coating were approximately 0.7 in the wavelength range of 0.25 μm to 7.0 μm, which is the spectral range that corresponds to the bandgap energy of the TPV cells. Little change in emissivity was observed after vacuum annealing of the ZYH coatings. Since the emissivity values for the ZYH coating are much less than Poco graphite and lower than 0.8, the ZYH coating is not the best candidate for TPV radiator applications. The ZTY coating had much higher emissivity values and contained a substantial amount of TiO_2, which indicates that ZrO_2-based coatings that contain TiO_2 have higher emissivity values compared to coatings that only contain Y_2O_3. The ZYH coatings exhibited excellent thermal stability after vacuum annealing at 1100°C to 1500°C and coating/substrate interactions were not observed.

Fe_2TiO_5 and $ZrTiO_4$ Coatings

Figure 5 shows that the as-deposited emissivity values for the $ZrTiO_4$ coating are significantly higher than Poco graphite. A large initial decrease in emissivity was observed in the first 500 hours of vacuum annealing of the $ZrTiO_4$ coatings (0.88-0.87 for as-deposited to 0.77-0.75 after 1100°C/500h vacuum anneal), followed by no change in emissivity with further annealing (0.77-0.75 for 1100°C/500h to 0.80-0.75 after 1100°C/4000h).

The $ZrTiO_4$ coatings were observed to exhibit a large initial weight loss followed by little weight change with vacuum annealing at 1100°C to 1500°C. Oxidation and volatilization of the molybdenum or niobium substrate particles could produce the large initial weight loss, and contribute to the low post-anneal emissivity values. XRD analysis indicates that the as-deposited coating was composed primarily of $ZrTiO_4$. Post anneal XRD indicated that little $ZrTiO_4$ was present, and the coatings contained larger amounts of ZrO_2. The $ZrTiO_4$ coating contains about 50% TiO_2, and evaporation of TiO_2 may also contribute to the large initial weight loss (Table I) and the large initial decrease in emissivity observed after vacuum annealing. Metallographic examinations show that a higher amount of porosity was observed in the $ZrTiO_4$ coating after vacuum annealing at 1200°C, which probably results from evaporation of TiO_2. The ZTY coating, which had excellent thermal stability with no change in emissivity values, contained a lower amount of TiO_2 (18%) and also contained Y_2O_3. These results indicate that ZrO_2-based coatings should not contain high amounts of TiO_2, and Y_2O_3 is needed to improve thermal stability and maintain high emissivity values.

The as-deposited emissivity values for the Fe_2TiO_5 coating were also significantly higher than Poco graphite. A large decrease in emissivity was observed in Figure 5 after vacuum annealing of the Fe_2TiO_5 coating. Large weight losses were also observed after vacuum annealing of the Fe_2TiO_5 coating. Post-anneal SEM and XRD analysis showed that the Fe_2O_3 was removed from the coatings, as Fe_2O_3 has a high vapor pressure under vacuum conditions at 1100°C, see Table I. The Fe_2TiO_5 coating has poor thermal stability due to Fe_2O_3 evaporation, which produces the large decreases in emissivity with vacuum annealing. The large coating weight losses and large amount porosity were observed metallographically after the first 500-1000 hours of vacuum annealing at 1200°C to 1500°C. Low weight changes and little increase in the amount of porosity were observed after annealing times of 1000 hours to 6000 hours at 1200°C to 1500°C. Coating/substrate interactions were not observed. This indicates that the initial large weight loss and decrease in emissivity observed for the Fe_2TiO_5 coating results from Fe_2O_3 evaporation, and the TiO_2 component of the Fe_2TiO_5 coating was fairly stable.

The post anneal emissivity values for the $ZrTiO_4$ and Fe_2TiO_5 coatings are significantly less than Poco graphite and lower than 0.8, which indicates that the $ZrTiO_4$ and Fe_2TiO_5 coatings are not the best materials for TPV radiator applications.

Coatings Deposited on Haynes 230

Large weight losses and significant degradation of the Haynes 230 base metal was observed during vacuum annealing at 1100°C. Haynes 230 contains high levels of chromium (20 to 23 weight %), and oxidation to form a chromia (Cr_2O_3) scale followed by volatilization by the formation of CrO_3 gas species during vacuum annealing produces large weight losses [1]. Due to the inherently poor thermal stability of Haynes 230 at 1100°C in vacuum, the thermal stability of the coatings deposited on Haynes 230 could not be evaluated.

CVD Rhenium Whisker Coatings

As-received emissivity values for the rhenium whisker coating were lower than values for Poco graphite but generally higher than 0.8, see Table II. Spectral emissivity results indicates that these coatings are graybody emitters. The emissivity values were varied with the CVD deposition time and conditions [1]. Vacuum annealing at 1100°C for 500 hours resulted in a significant decrease in emissivity from 0.8 for as-deposited to 0.69. This indicates that rhenium whisker coatings in their current form do not have the desired thermal stability for TPV radiator applications.

Summary and Conclusions

The emissivity results for the coatings evaluated in this work are summarized in Table II. Only the ZrC, ZTY, and $Al_2O_3 - TiO_2$ coatings have post-anneal values greater than 0.8. These coatings are basically graybody emitter coatings, with relatively constant emissivity values over the wavelength range that matches the above bandgap energy of TPV cells. The highest emissivity values are observed for the $Al_2O_3 - TiO_2$ coatings, followed by the ZTY and ZrC coatings. The ZTY coating exhibited the best thermal stability, while the thermal stability of the $Al_2O_3 - TiO_2$ and ZrC coatings in vacuum conditions at temperatures of 1200°C or less was excellent.

Acknowledgements

This work was preformed under USDOE Contract DE-AC11-98PN38206. The useful comments, discussion and contributions from D.P. Measures and W.L. Ohlinger are appreciated. The support of various Bettis personnel in completing this work is also appreciated (J.E. Sundin, R.K. Ramaley, T.A. Dobrich, D.M. Gasparovic, A. Stinson, and D.L. Ward). Thanks to R.A. Douty and D.G. Sinchar for producing the LPPS $Al_2O_3 - TiO_2$ coatings.

References

1. B.V. Cockeram, D.P. Measures, and A.J. Mueller, "The development and testing of emissivity enhancement coatings for thermophotovoltaic (TPV) radiator applications", Thin Solid Films, 355/356 (1999), 17-25.
2. S.K. Rutledge, M.J. Forkapa, and J.M. Cooper, "Thermal Emittance Enhancement of Graphite-Copper Composites for High Temperature Space Based Radiators" (NASA-TM-105178, 1991).
3. R. Siegel and J.R. Howell, Thermal Radiation Heat Transfer, 3rd edition (Washington, DC, Hemisphere, 1992).
4. M.J. Mirtich and M.T. Kussmaul, "Enhanced Thermal Emittance of Space Radiators by Ion Discharge Chamber Texturing" (NASA-TM-100137, 1987).
5. Y.S. Touloukian and D.P. Dewitt, Thermophysical Properties of Matter: Volume 8, "Thermal Radiative Properties of Nonmetallic Solids", (New York, IFI/Plenum, 1972).
6. A. Roine, HSC Chemistry for Windows, (PORI, Finland, Outokumpu Research Oy, 1999).
7. F.W. Sears and G.L. Salinger, Thermodynamics, Kinetic Theory, and Statistical Thermodynamics, 3rd edition, (New York, New York, Addison Wesley, 1975).
8. M. W. Chase et al., eds., JANEF Thermodynamical Tables, 3rd edition, J. Phys. Chem. Ref. Data, vol. 14 (1985).

Table I. Summary of thermodynamic calculations of the highest vapor pressure for various coating materials (under conditions of 1 ppm O_2 + 1ppm H_2O at 1100°C and 10^{-6} atm pressure). The vaporization rate (G) is also determined using Eq. (3) with α=1.

Coating Material	Vapor Species with highest partial pressure / and values of equilibrium partial pressure	Vaporization rate, G [g / cm^2 - s]
ZrC	ZrO – 8.7 X 10^{-9}	1.13 X 10^{-7}
ZrO_2	ZrO_2 – 1.6 X 10^{-14}	2.09 X 10^{-13}
TiO_2	TiO_2 – 6.2 X 10^{-9}	6.63 X 10^{-8}
Y_2O_3	YO_2 – 5.5 X 10^{-9}	7.27 X 10^{-8}
Fe_2O_3	FeO – 1.5 X 10^{-6}	1.48 X 10^{-5}
Al_2O_3	AlO(OH) – 1.7 X 10^{-13}	1.56 X 10^{-12}

Table II. Summary of emissivity results (pre- and post-anneal) for enhancement coatings of a TPV radiator, with a comment on thermal stability. The coating candidates are listed in order of preference. Results for as-received Poco graphite are included for comparison.

Coating Candidate	Emissivity		Thermal Stability
	As-received	Post-anneal [1100°C/4000h]	
Al_2O_3 / TiO_2 coatings	0.88 – 0.96	0.88 – 0.93	Excellent thermal stability at T < 1350°C.
ZrO_2 + 18% TiO_2 + 10% Y_2O_3 coatings	0.86 – 0.89	0.87	Excellent thermal stability at T < 1350°C. Lower weight losses than observed for Al_2O_3 / TiO_2 coatings.
ZrC coatings	0.89 – 0.91	0.83	Larger initial weight loss observed in the first 500 hours of annealing from limited oxidation of the ZrC coating. Excellent thermal stability between 500 to 6000 hours of vacuum annealing.
$ZrTiO_4$ coatings	0.87 – 0.89	0.75 – 0.79	Excellent thermal stability at T < 1350°C. Large initial weight loss observed followed by low weight changes.
ZrO_2 + 8% Y_2O_3 + 2% HfO_2 coatings	0.75 – 0.85	0.72	Best thermal stability of all coatings. Excellent thermal stability at T < 1500°C.
CVD Rhenium Whiskers	0.73 – 0.86	0.69	Low post-anneal emittance value observed.
Fe_2TiO_5 coatings	0.89 – 0.93	0.73 – 0.81	Poor thermal stability due to high vaporization rate of Fe_2O_3.
Poco Graphite (as-received)	0.86	N/A	N/A

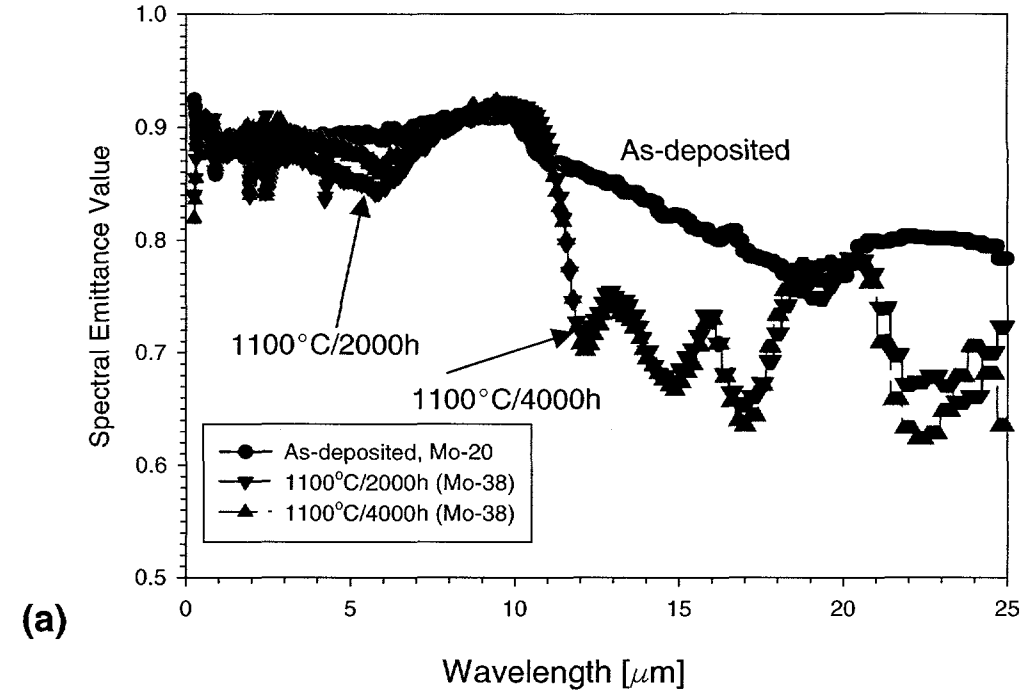

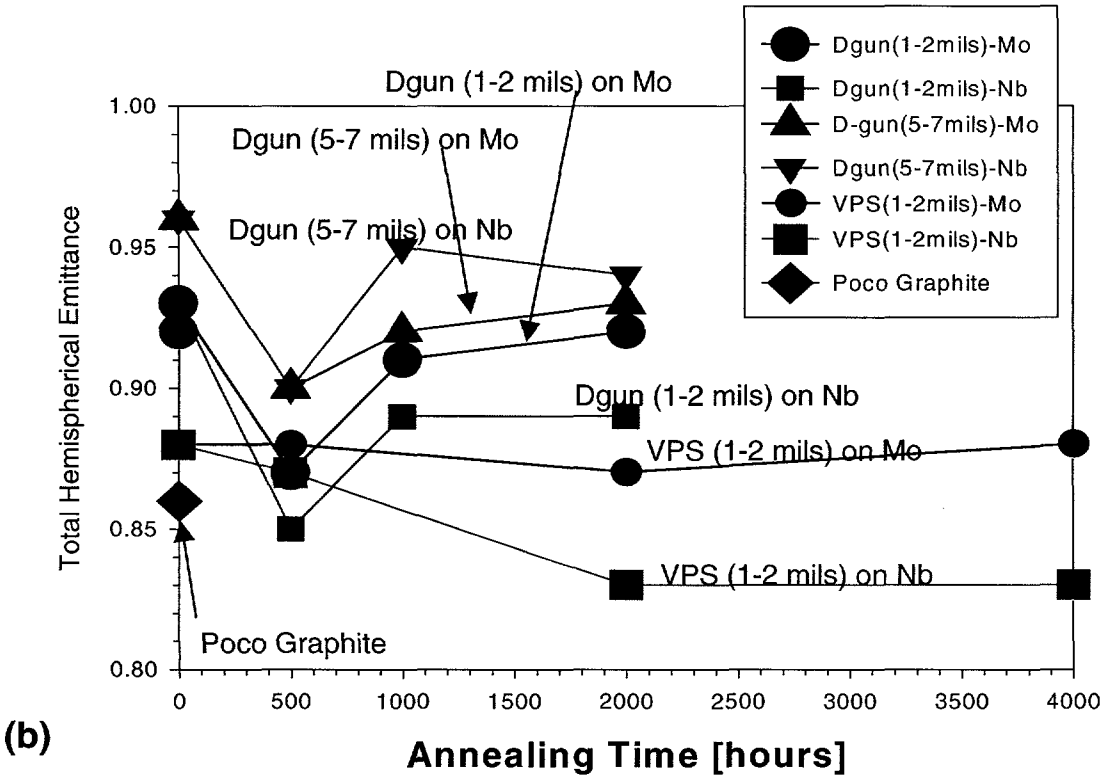

Figure 1. Emissivity values for VPS and D-gun Al_2O_3 – TiO_2 coatings: (a) spectral emissivity values for VPS coatings deposited on molybdenum in as-deposited and post-annealed condition, and (b) total hemispherical emittance values determined at 1400K at NASA-GRC for VPS and D-gun coatings versus annealing time. As-deposited values are shown at the 0 hours annealing time. Data for as-received Poco graphite is shown in Figure 1b (black diamond).

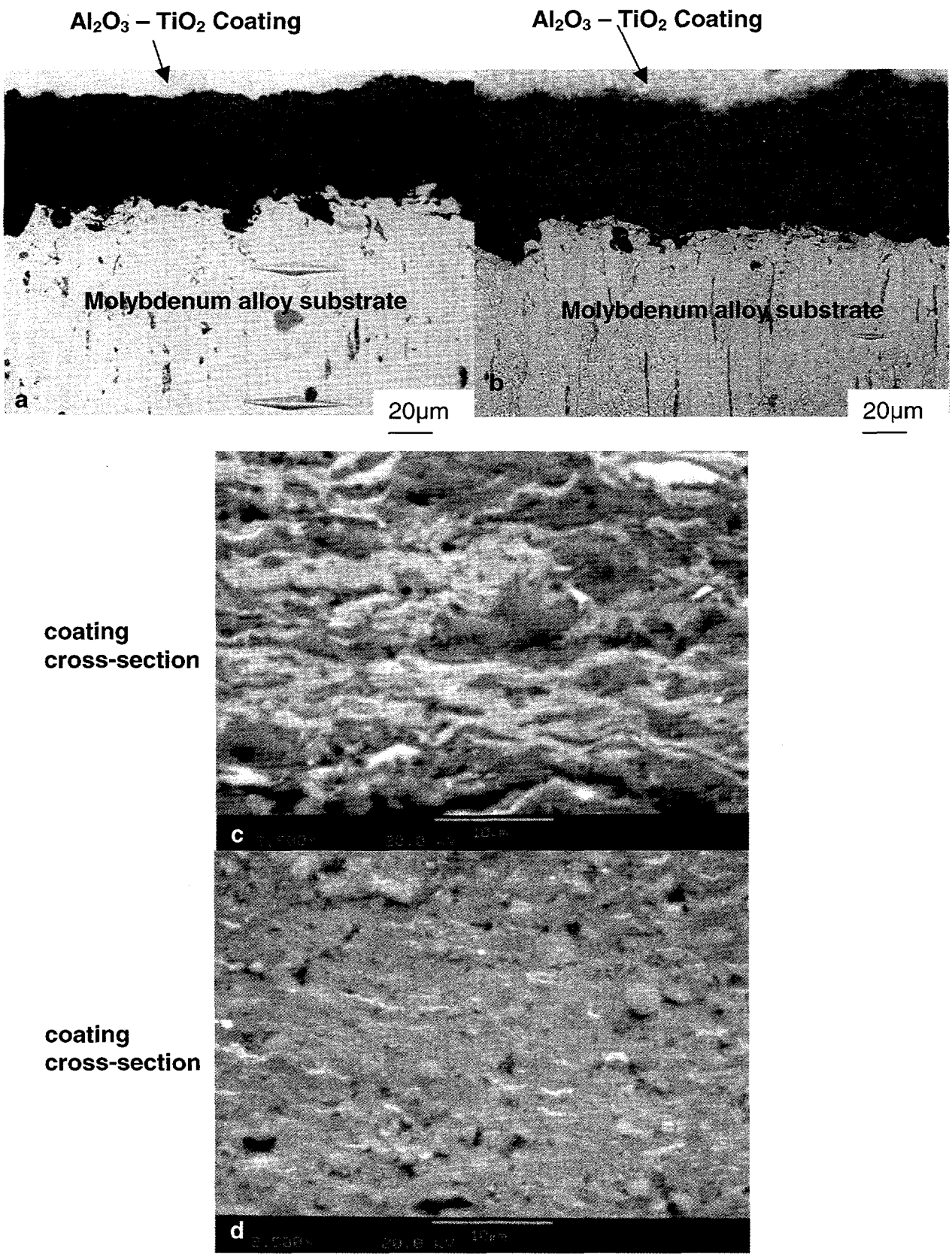

Figure 2. Metallographic cross-sections of the $Al_2O_3 - TiO_2$ coatings: (a) D-gun coating deposited on a molybdenum alloy after a 1200°C / 1000 hour vacuum anneal, (b) D-gun coating deposited on a molybdenum alloy after a 1200°C / 6000 hour vacuum anneal, (c) LPPS $87Al_2O_3$ / $13TiO_2$ coating deposited on molybdenum (as-deposited condition), and (d) LPPS $90Al_2O_3$ / $10TiO_2$ coating deposited on molybdenum in as-deposited condition. The indents in Figures 2a and 2b were made at different loads.

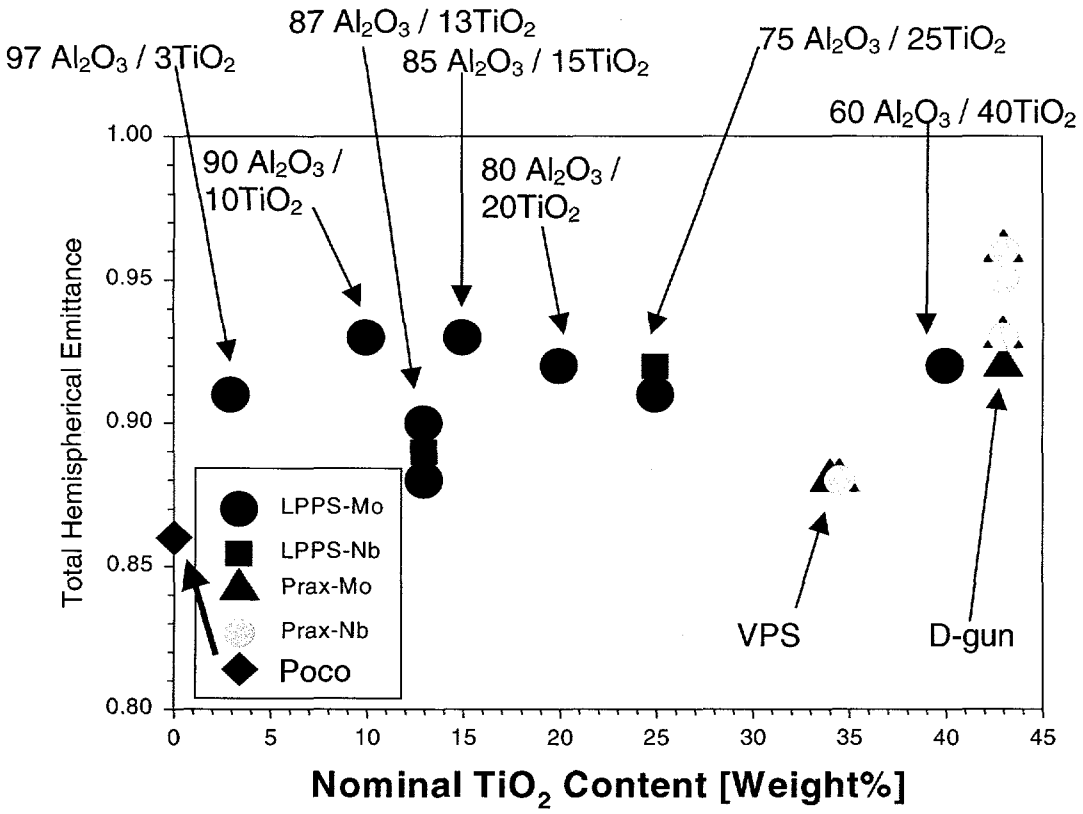

Figure 3. Plot of total hemispherical emittance versus nominal TiO_2 content (in weight %) for the LPPS Al_2O_3 / TiO_2 coatings deposited on molybdenum (blue circles) and niobium (green square) substrates compared with data for VPS and D-gun coated molybdenum (dark red triangle) and niobium (gray circle) substrates. Results for Poco Graphite (Black diamond) are also shown. All coatings are in the as-deposited condition. The nominal compositions for the Praxair coatings were determined from microprobe analysis.

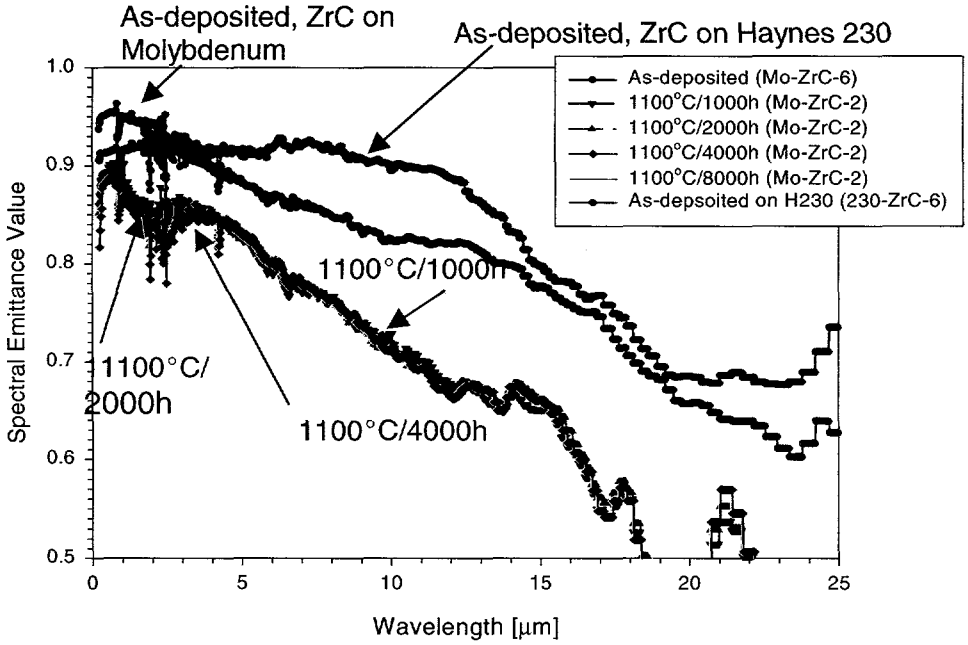

Figure 4. Spectral emittance values measured at NASA-GRC for VPS ZrC coatings deposited on molybdenum and Haynes 230. For the ZrC coatings deposited on molybdenum, spectral emittance values for an as-deposited coupon (red circles) are compared with a companion coupon (Mo-ZrC-2) after annealing at 1100°C for 1000h (blue inverted triangles), 1100°C for 2000h (green triangles), and 1100°C for 4000h (black diamonds). Spectral emittance values are shown for a ZrC deposited on Haynes 230 in the as-deposited condition (dark red circles).

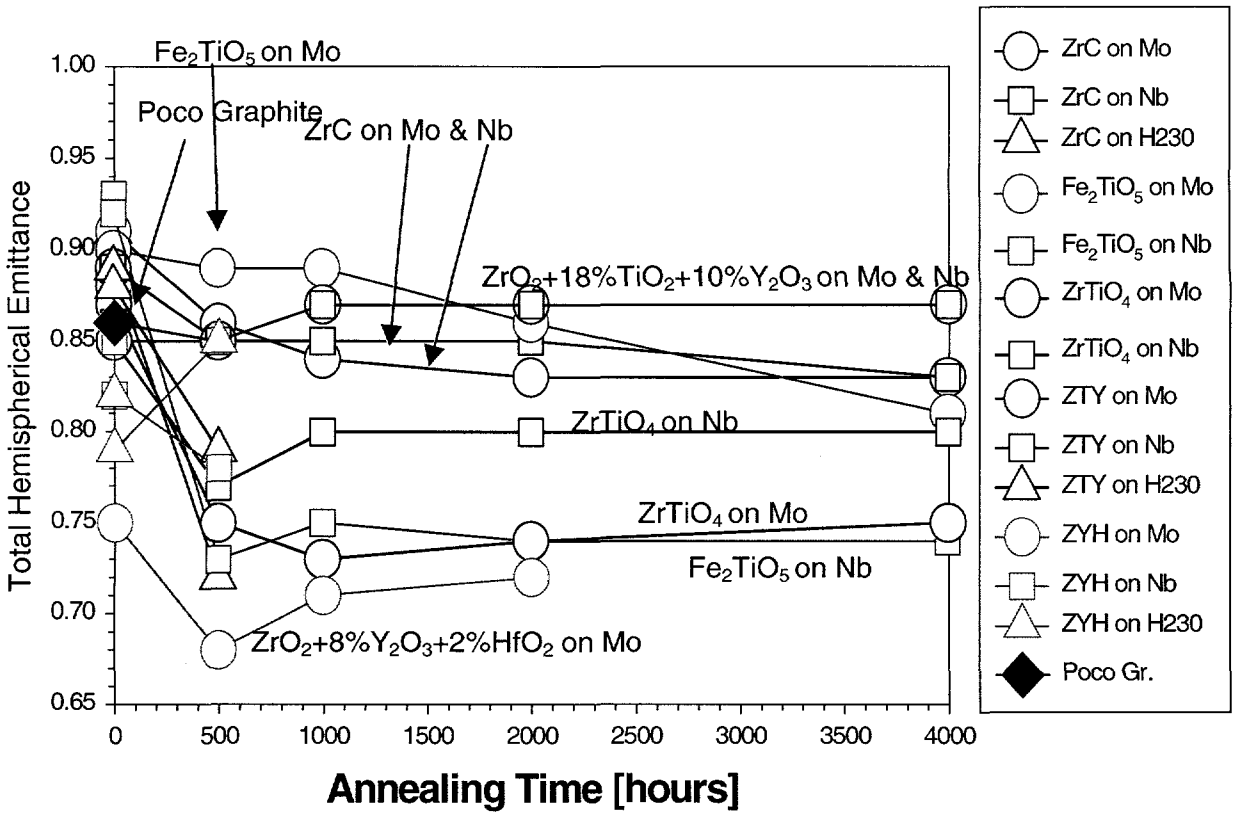

Figure 5. Plot of total hemispherical emittance values measured at 1400K at NASA-GRC versus annealing time for the various VPS coatings from SUNY. Results are shown for coatings deposited on molybdenum (circles), niobium (squares), and Haynes 230 (triangles). The SUNY VPS coatings are ZrC (blue color), Fe_2TiO_5 (green color), $ZrTiO_4$ (red color), ZrO_2+18%TiO_2+10%Y_2O_3 (dark red color), and ZrO_2+8%Y_2O_3+2%HfO_2 (dark yellow). As-deposited values are shown at the 0 hours annealing time. Data for Poco graphite is shown (black diamond) for comparison.

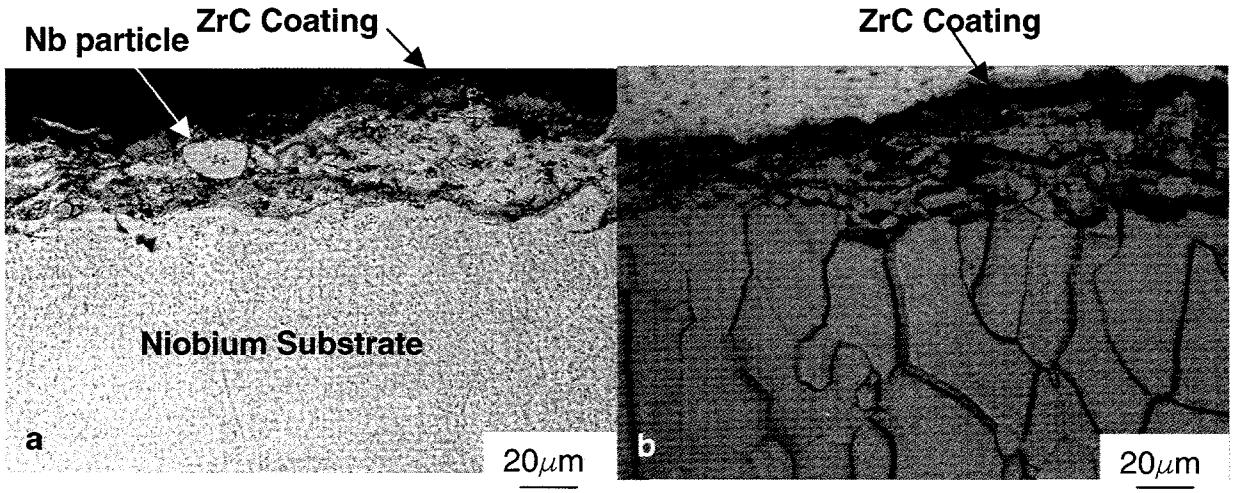

Figure 6. Metallographic cross-sections of VPS ZrC coating: (a) ZrC coating deposited on niobium (as-deposited condition), and (b) ZrC coating deposited on molybdenum after 1200°C vacuum anneal for 6000 hours.

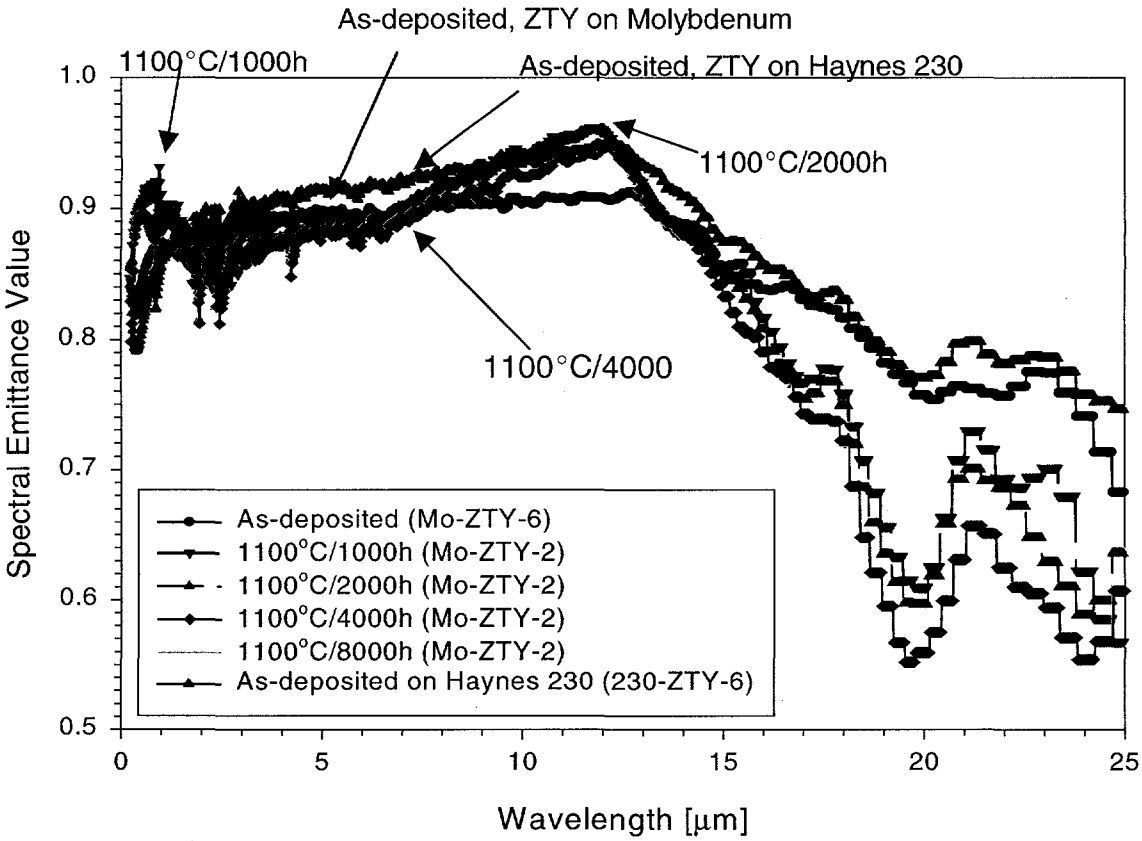

Figure 7. Spectral emittance values measured at NASA-GRC for SUNY VPS ZrO_2 + 18% TiO_2 + 10% Y_2O_3 (ZTY) coatings deposited on molybdenum and Haynes 230. For the coatings deposited on molybdenum, spectral emittance values for an as-deposited coupon (red circles) are compared with a companion coupon (Mo-ZTY-2) after annealing at 1100°C for 1000h (blue inverted triangles), 1100°C for 2000h (green triangles), and 1100°C for 4000h (black diamonds). Spectral emittance results are shown for an as-deposited coating on a Haynes 230 substrate (dark red triangle, 230-ZTY-6).

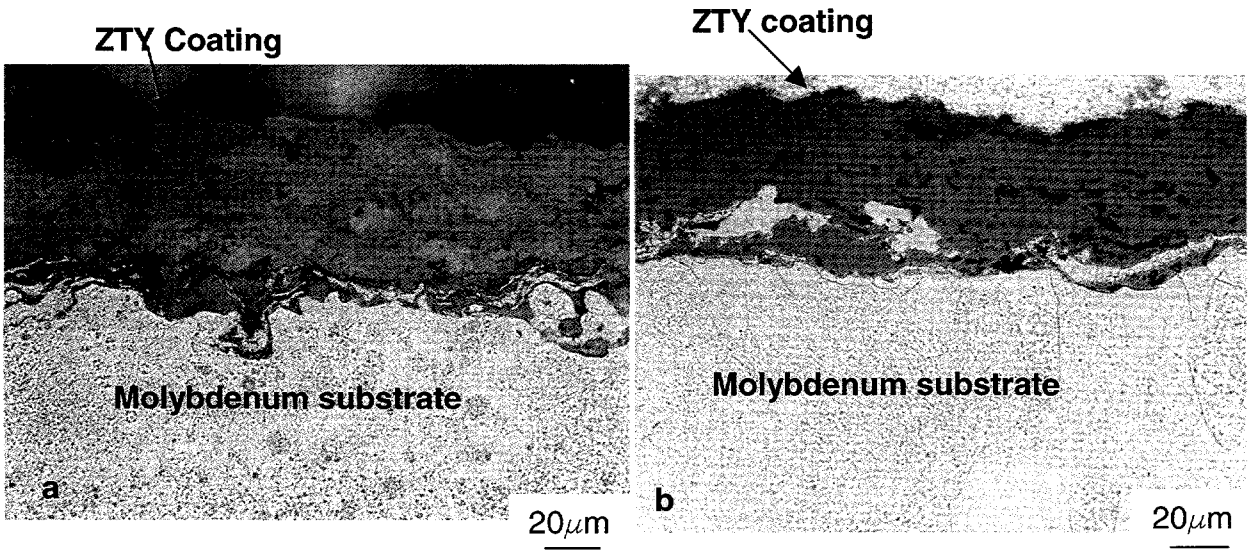

Figure 8. Metallographic cross-sections of SUNY VPS ZrO_2 + 18% TiO_2 + 10% Y_2O_3 (ZTY) coatings: (a) as-deposited coating on molybdenum, and (b) coating deposited on molybdenum after 6000 hour vacuum anneal at 1200°C.